

Resonance positions and lifetimes for flexible complex absorbing potentials

Roland Lefebvre,^{*} Milan Sindelka,[†] and Nimrod Moiseyev[‡]

Department of Chemistry and Minerva Center of Nonlinear Physics in Complex Systems, Technion—Israel Institute of Technology, Haifa 32000, Israel

(Received 13 June 2005; published 7 November 2005)

By adding *any* complex absorbing potential (CAP) $-i\lambda V(\vec{r})$ to a system Hamiltonian, the corresponding complex eigenvalues are analytical functions of λ , $E_j(\lambda)$. It is shown here that for a quite general flexible class of CAP's the real part of $\lim_{\lambda \rightarrow 0} E_j(\lambda)$ provides the resonance energy. The imaginary part of that limit is the resonance width (i.e., inverse lifetime) in spite of the fact that $\text{Im } E_j(0)=0$. The need for the Padé approximation within this approach is explained. Application to an illustrative numerical test case model Hamiltonian is given. This method could open a gate for studying systems that could not be studied until now due to the complexity of the numerical computations. In particular, one may in this way obtain resonance energies by a modification, in a straightforward simple manner, of the widely used conventional methods that were developed for the calculations of bound states.

DOI: 10.1103/PhysRevA.72.052704

PACS number(s): 03.65.Nk, 05.60.Gg, 61.14.Dc

I. INTRODUCTION

The resonance phenomenon appears in many different fields of physics, chemistry, and technology. Let us briefly mention α and β radioactive decay, atomic and molecular autoionization, Auger spectroscopy, shape and Feshbach resonances, the predesorption of atoms and molecules from solid surfaces, above-threshold ionization, high-order harmonic generation of atoms and molecules in strong laser fields, and resonance tunneling transistors and diodes. Another example is the recent prediction of the intra-Coulombic-decay phenomena [1] which have been confirmed by experiments [2]. In order to guide the experiments there is also the need for the calculation of resonance complex-energy surfaces to high accuracy [3]. As a last example we can quote the calculation of resonance energies for nuclear systems decaying via a three-body mechanism [4].

Resonance energies and lifetimes are associated with the real and with the inverse of the imaginary parts of the complex eigenvalues of the Schrödinger equation. Complex eigenvalues are obtained by imposing outgoing boundary conditions on the corresponding eigenfunctions. The consequence of these boundary conditions is that the resonance wave functions diverge exponentially [5,6]. A common way to deal with this problem is to introduce complex absorbing local potentials (CAP's) on the edge of the grid. This approach has been borrowed [7] from nuclear physics [8,9] and can be applied to both scattering and resonance problems. See for example [10] for an application to resonances. A recent review on the use of CAP's is in [11] with

references therein. For resonances this is made with two purposes: (i) to make the wave function square integrable; (ii) to avoid the reflection of running waves by the edge of the grid which is used in the numerical calculation. Reflection-free CAP's have been devised in [12,13]. It has been proven [12] that such CAP's are associated with complex scaling transformations that stand on a rigorous mathematical ground [14–18]. Unfortunately they are not easy to implement for large and complex systems. The flexible CAP's which are used in the present study are not reflection-free potentials. They do not require the careful tailoring which is generally both energy and range dependent (see for example [19–21] for the case of a linear CAP). However it will be shown that they can provide the desired information about resonances, up to all significant digits of accuracy.

More than a decade ago it has been proposed [22] to calculate resonance energies by the multiplication of the Planck constant by $\exp(-i\phi)$ or the reduced mass by $\exp(2i\phi)$. Such modifications produce a Hamiltonian which for a one-dimensional situation is given by

$$H(r, \phi) = -\frac{\hbar^2}{2m} \exp(-2i\phi) \frac{\partial^2}{\partial r^2} + V(r). \quad (1)$$

For a vanishing asymptotic potential, the outgoing solution is of the form $\exp(i\tilde{k}r)$, with a modified wave number \tilde{k} given by

$$\tilde{k}^2 = \frac{2mE}{\hbar^2} \exp(2i\phi). \quad (2)$$

The result is to induce a positive imaginary part in the asymptotic wave number which in turn produces a damping of the wave function. With the help of the Padé procedure, the extrapolation of the complex eigenvalues obtained for $\phi \neq 0$ to $\phi=0$ gives the resonance position and lifetime. The present study goes along similar lines (cf. also [23]). A CAP of the form $V_{CAP} = -i\lambda r^N$ for a one-dimensional system, with $N > 0$, is added to the Hamiltonian. The “puzzle” is as follows: how does it come that by using a Padé approximant to

^{*}Permanent address: Laboratoire de Photophysique Moléculaire du CNRS, Université de Paris-Sud, 91405 Orsay, France and U.F.R. de Physique Fondamentale et Appliquée, Université Pierre et Marie Curie, 75231 Paris, France. Electronic address: roland.lefebvre@ppm.u-psud.fr

[†]Email address: chmilan@technix.technion.ac.il

[‡]Email address: nimrod@technix.technion.ac.il

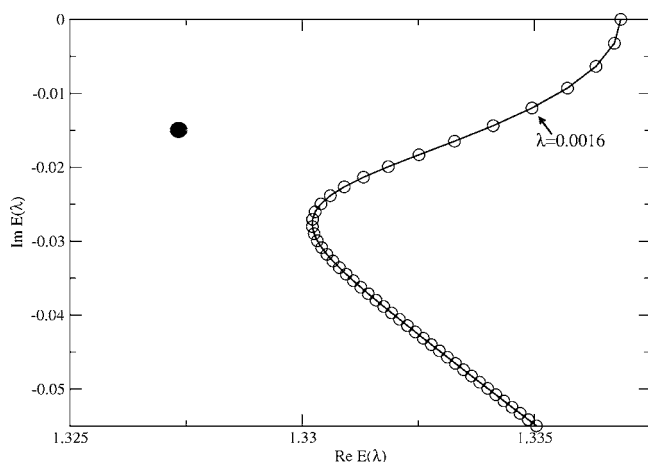


FIG. 1. The complex eigenvalues as functions of λ , as obtained for the test-case study problem using 500 particle-in-a-box basis functions (the box size is $L_{\text{box}}=30$ a.u.). The parameter λ was given the values $\lambda_j=0.0004(j-1)$. Results differing by $\Delta\lambda=0.004$ are shown as open circles. One representative value of λ is shown. The full circle stands for the results obtained from the application of the Padé-approximation-extrapolation procedure.

compute $\lim_{\lambda \rightarrow 0} E(\lambda)$ the resonance complex eigenvalue is obtained rather than the real eigenvalue which has been calculated for $\lambda=0$?

Let us first introduce the puzzle by an illustrative numerical example. In Sec. III the solution is presented, supported by a proof that with any $V_{\text{CAP}}=-i\lambda r^N$ added to the Hamiltonian, the resonance wave functions become square integrable. We show that this statement holds for any value of $\lambda \neq 0$ when $N > 0$. However, the resonance wave functions decay and vanish exponentially at the edge of the grid only for $\lambda \geq \lambda_c$ where the critical value of λ is basis-set or grid dependent. As the basis set is closer to completeness or the grid gets larger λ_c gets smaller values. We then explain why, with the help of the Padé approximation, the resonance positions and widths can be computed. In Sec. IV we apply the method presented in this paper to cases where a Gaussian basis set is used. The ability of using a Gaussian basis set in applying the method presented here is very important in view of its possible use in electronic structure calculations of many electron systems. In Sec. V we conclude.

II. THE PUZZLE

As a test-study model Hamiltonian we have chosen $\hat{H}(r) = -0.5d^2/dr^2 + (r^2/2 - 0.8)\exp(-0.1r^2)$ which has been used before to check new theories and computational methods for calculating resonances [24–27]. In this model Hamiltonian the potential consists of a well embedded between two potential barriers of equal heights. The potential supports only one bound state and two isolated narrow resonances that are located below the top of the potential barriers. In Fig. 1 we show the complex eigenvalues $E(\lambda)$ that were obtained for the highest of the two resonances from the diagonalization of a complex symmetric 500×500 matrix. The associated wave function is symmetric with respect to inversion. The matrix

elements are given by $H_{\text{CAP}}(i,j) = \langle i | \hat{H}(r) - i\lambda r^2 | j \rangle$ where $|i\rangle$ and $|j\rangle$ are particle-in-a-box functions. Here the box size is $L_{\text{box}}=30$ a.u. Six-figure accuracy is required. A continuous curve is obtained for $E(\lambda)$ where $\text{Im}[E(\lambda)]=0$ for $\lambda=0$. Ten values of $E(\lambda)$ are selected for $\lambda_j=0.004+0.0002(j-1)$ where $j=1,2,\dots,10$. These values are used to build the Padé approximant

$$E_{\text{Padé}}(\lambda) = \frac{\sum_{j=0}^4 p_j \lambda^j}{1 + \sum_{i=1}^4 q_i \lambda^i} \quad (3)$$

such that

$$E(\lambda_j) = E_{\text{Padé}}(\lambda_j). \quad (4)$$

For more information on the use of Padé approximants see [22,28]. The extrapolation to $\lambda=0$ provides the result that is labeled by a full circle in Fig. 1,

$$\lim_{\lambda \rightarrow 0} E_{\text{Padé}}(\lambda) = p_0 = 1.327\,212 - i0.015\,448\,1 \quad (5)$$

while complex rotation provides $1.327\,197 - i0.015\,447\,3$ [24]. The puzzle is clear. Why does the Padé approximant provide a point which is not embedded on the curve $E(\lambda)$? How does it come about that the resonance position and width (inverse lifetime) are obtained with such high accuracy?

III. THE SOLUTION OF THE PUZZLE AND ITS IMPLICATION FOR NUMERICAL CALCULATIONS OF RESONANCES

As a step toward the solution of the puzzle we present in Fig. 2 the complex eigenvalues as functions of the CAP strength parameter λ for two box sizes: $L_{\text{box}}=30$ a.u. (the previous calculation) and $L_{\text{box}}=40$ a.u. The parameter λ is given values $0.0002(i-1)$ where $i=1,2,\dots,151$. The solid line which is shown in Fig. 2 describes the corresponding complex eigenvalues that would be obtained if there was no constraint due to the finiteness of the box size. These are called the “numerically exact values.” It is important to note that these values are obtained by applying the complex scaling transformation to the Hamiltonian with a CAP, i.e., when $\hat{H}(r) \rightarrow \hat{H}(r \exp(i\theta)) - i\lambda r^N \exp(i\theta N)$. Upon complex scaling the resonance wave functions become well localized in space (i.e., square integrable) even for $\lambda=0$. The numerical exact results are compared with the results obtained when $\hat{H}(r) \rightarrow \hat{H}(r) - i\lambda r^N$ (no complex scaling transformation is applied here). As one can see from Fig. 2, for sufficiently large values of λ the results obtained for the different basis sets coalesce with the exact numerical values. The coincidence for $\lambda \geq \lambda_c$ is due to the fact that we are dealing with bound states in both cases (with and without complex rotation) and that although here the eigenvalue is complex, it is known that complex rotation does not affect bound states eigenvalues. Moreover, the critical value of λ for which

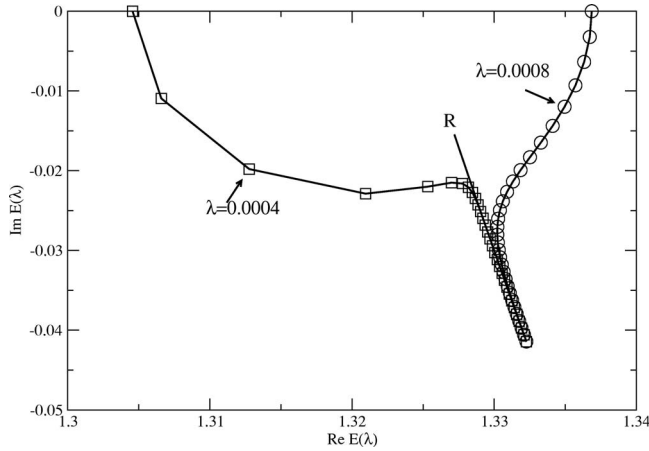


FIG. 2. The complex eigenvalues for CAP strength parameters $\lambda_j=0.0002(j-1)$ that were obtained from the diagonalization of a 500×500 complex symmetric matrix. Two types of particle-in-a-box basis functions are used. One set of basis functions is associated with a box size $L_{box}=30$ a.u. and produces the energies shown by the open circles. The other set of energies shown by the open squares are associated with $L_{box}=40$ a.u. The arrows select representative values of λ . The solid line describes the so-called numerically exact results described in the text. R stands for the resonance position.

$$|E_{basis\ set}(\lambda > \lambda_c) - E_{exact}(\lambda)| = \epsilon, \quad (6)$$

where ϵ is practically equal to zero (i.e., all significant digits are zero), depends on the set of basis functions used in the calculation. As L_{box} gets a larger value, provided a large enough number of basis functions is used to get converged results, the value of λ_c is smaller. Figure 3 gives additional evidence of this behavior for a linear CAP and a propagation technique which allows one to go to extremely large box sizes. This shows that as the basis set gets closer to completeness the numerical exact complex eigenvalues will be obtained even for infinitesimally small values of λ . This is an interesting result. Within the framework of the complex scaling method a resonance wave function becomes square integrable *only* when the scaling parameter (i.e., rotational angle θ) gets values that are larger than a critical value θ_c given by (for a zero threshold energy) $\tan(\theta_c) = -\text{Im } E_{res} / \text{Re } E_{res}$ (see the reviews in [16,18]). In contrast the critical value of the relevant parameter in the present approach can go to zero. Later we will discuss the fact that the quadratic CAP $-i\lambda r^2$ changes the asymptote of the resonance wave function to be a square-integrable function in a way very similar to that suggested before by Zel'dovich and his co-workers [6].

The answer to the question of why by using Padé approximants we get the resonance complex eigenvalue rather than the real eigenvalue that was obtained in our numerical calculation when $\lambda=0$ is as follows: when $\lambda \geq \lambda_c$ and Eq. (6) holds, the Padé approximation cannot be sensitive to the differences (if any) between the complex eigenvalues which were obtained by either the CAP with $\lambda \geq \lambda_c$ or with these same values of λ and complex rotation. Another way of asking the question is this: Why does the extrapolation by the Padé method give the value of $E_{exact}(\lambda=0) \equiv E_{res}$ and not the

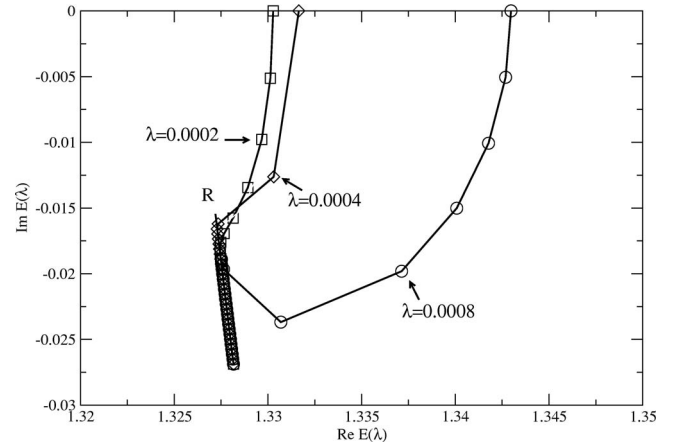


FIG. 3. The complex eigenvalues as functions of the strength parameter $\lambda_j=0.0002(j-1)$ of a linear CAP with $j=1,2,\dots,151$. Three box sizes are used: $L_{box}=160$ (circles), 200 (squares), and 400 (diamonds) in a.u. A propagation+matching technique determines the energies. Note the kink along the curve for $L_{box}=160$. All curves merge finally with the almost straight line leading to the resonance position. The larger the box size, the sooner the merging occurs. The arrows select representative values of λ . A Padé approximant is to be built on the energies belonging to the straight line. These energies do not depend on the box size. The approximant generates the resonance energy symbolized by R .

value of $E_{basis\ set}(\lambda=0)$ which is a real number? The information about “kinks” and other abrupt changes of $E(\lambda < \lambda_c)$ is embedded in the high-order derivatives of $E(\lambda \geq \lambda_c)$. Using a first-order perturbation argument we will show below that $E_{exact}(\lambda) \sim E_{res} + \lambda \Delta E$. The extrapolation to $\lambda=0$ follows the smooth linearly λ -dependent function and the resonance complex eigenvalue is obtained. This is the explanation to the puzzle as presented in Sec. II.

A simple argument showing that when CAP's of the form $-i\lambda r^{N>0}$ are included in the Hamiltonian the resonance wave functions become square integrable can be given within the semiclassical approach. The semiclassical wave function with outgoing behavior can be written

$$\Psi(r) \sim \frac{1}{\sqrt{k(r)}} \exp\left(i \int^r k(r') dr'\right). \quad (7)$$

The local wave number $k(r)$ is

$$k(r) = [2m(E - V(r) + i\lambda r^N)]^{1/2}. \quad (8)$$

For large r , for the calculation of the integral, we approximate $k(r)$ as

$$k(r) \sim \sqrt{2m(i\lambda r^N)}^{1/2} = (1+i)(m\lambda)^{1/2} r^{N/2}. \quad (9)$$

This gives

$$\int^r k(r') dr' \sim \frac{2}{N+2} (m\lambda)^{1/2} (1+i) r^{(N+2)/2}. \quad (10)$$

The introduction of this integral and of the local wave number into the semiclassical form of $\Psi(r)$ gives

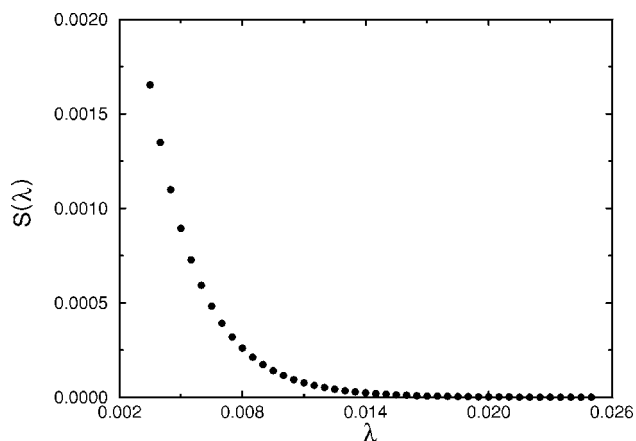


FIG. 4. The integral $S(\lambda) = |\int_{10}^{L_{\text{box}}=20} \Psi_{\text{CAP}}^2(x; \lambda) dx|$ as a function of λ when 500 particle-in-a-box basis functions have been used as a basis set.

$$\Psi(r) \sim (m\lambda)^{-1/4} (1+i)^{-1/2} r^{-1/4} \exp\left(+\frac{2i}{N+2} (m\lambda)^{1/2} r^{(N+2)/2}\right) \times \exp\left(-\frac{2}{N+2} (m\lambda)^{1/2} r^{(N+2)/2}\right). \quad (11)$$

The second exponential factor ensures asymptotic damping for any real positive value of N with $N > 0$. The case for $N=1$ is treated more fully in the Appendix. As λ gets smaller values the suppression of the natural exponential growth of the resonance wave function happens at larger distances from the origin. Therefore, for a given basis set the suppression of this growth happens when λ gets values which are *larger* than a critical value. In Fig. 4 we present the integral $S(\lambda) = |\int_{10}^{L_{\text{box}}=20} \Psi_{\text{CAP}}^2(x; \lambda) dx|$ as a function of λ when 500 particle-in-a-box basis functions have been used. As one can see the wave function becomes localized in the interaction region when $\lambda > \lambda_c \sim 0.014$. This value of λ_c is in good agreement with the results presented in Fig. 2.

In this context we should mention the Zel'dovich normalization of resonance wave functions. To make the resonance wave function square integrable, Zel'dovich [6] suggested multiplying the resonance wave functions by a Gaussian $\exp(-\sigma r^2)$, where after the calculations of expectation values the limit of $\sigma \rightarrow 0$ is carried out; namely, the inner product is defined not as $(\Psi_{\text{res}} | \Psi_{\text{res}})$ but as $(\Psi_{\text{res}} | \exp(-\sigma r^2) | \Psi_{\text{res}})$ when $\sigma \rightarrow 0^+$. Our results for a quadratic CAP are in this spirit as one can see from Eq. (11) with $N=2$, where $\frac{1}{2}(m\lambda)^{1/2}$ stands for σ .

There are two additional aspects of the method which are worth explaining. One deals with a different way to calculate the energies called numerically exact in previous sections. The other is to account for the almost linear behavior with respect to λ when λ is close to zero. When $\lambda=0$ the exponential growth of the resonance wave function prevents the use of the basis set method. This problem is avoided if we complex scale the Hamiltonian $\hat{H}(r) - i\lambda r^N$ by $\exp(i\theta)$. In such a case for $\lambda=0$ we get the converged resonance complex eigenvalue. When $\lambda \neq 0$ the wave function is already a square-integrable function. These energies coincide numeri-

cally, as already stated, with those obtained for $\theta=0$ and $\lambda \geq \lambda_c$. These energies can also be obtained as Padé approximants starting from values of λ somewhere along the nearly straight line and extrapolating toward $\lambda=0$.

To explain the close-to-linear behavior we choose here as a zeroth-order Hamiltonian

$$\hat{H}_0 = \hat{H} - i\epsilon r^N, \quad (12)$$

where ϵ is taken as an arbitrarily small positive number, such that

$$\hat{H}_0 \Psi_{\text{res}} = E_{\text{res}} \Psi_{\text{res}}. \quad (13)$$

The perturbation is taken as $V_{\text{CAP}} = -i\lambda r^N$. The complex λ -dependent energy is given by

$$E_{\text{exact}}(\lambda) = E_{\text{res}} - i\lambda E_{\text{CAP}}^{(1)} + \sum_{n=2} (-i\lambda)^n E_{\text{CAP}}^{(n)}, \quad (14)$$

where

$$E_{\text{CAP}}^{(1)} = \int \Psi_{\text{res}}(r) r^N \Psi_{\text{res}}(r) dr. \quad (15)$$

It should be stressed that instead of the conventional scalar product we use here the so-called *c* product [24]. Because even with a very small ϵ the function $\Psi_{\text{res}}(r)$ decays exponentially [cf. Eq. (11)] the integral is finite. From this perturbational analysis it results that a nearly linear dependence of the complex eigenvalue associated with the resonance energy with respect to λ is expected. Figures 2 and 3 strongly support this conclusion.

IV. RESONANCES WITH THE HELP OF FLEXIBLE CAP'S WITH A GAUSSIAN BASIS SET

In order to apply the method presented here, i.e., calculating resonances by using flexible CAP's with the help of Padé approximants, to molecules or to many-electron quantum dots, it is very important to show that we can use Gaussian basis functions. Most if not all of the widely used packages for electron structure calculations incorporate Gaussian functions as a basis set in order to simplify the calculations of the Hamiltonian matrix elements. For the one-dimensional test-case study model Hamiltonian of the previous sections we use even-tempered Gaussians as a basis set. That is, $\phi_j(x) = \exp(-\alpha_j e^{j-1} x^2)$ where $j=1, 2, \dots, N$. In Fig. 5 we present the complex eigenvalues as obtained by solving the general eigenvalue problem $\det[\mathbf{H}_{\text{CAP}} - E(\lambda)\mathbf{S}] = 0$, where \mathbf{H}_{CAP} is the Hamiltonian matrix and \mathbf{S} is the Gaussian overlap matrix. Here 60 Gaussians were used as a basis set. The results presented in Fig. 5 clearly show that due to the use of the localized even-tempered Gaussian basis functions the complex eigenvalues are converged and become basis-set independent for $\lambda \geq \lambda_c$ when λ_c is about ten times larger than before when particle-in-a-box basis functions were used. The conclusion is clear. When Gaussian basis functions are used the method is applicable but the flexible CAP strength parameter should get sufficiently large values. The Padé procedure is applied to the energies calculated for $\lambda_j = 0.03 + j \cdot 0.0001$. The results

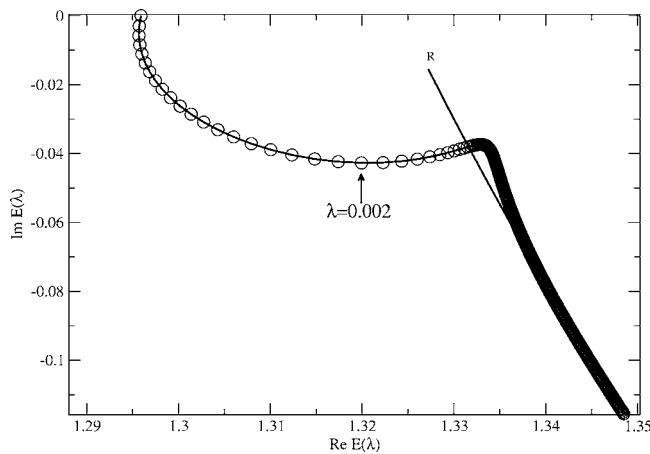


FIG. 5. The complex eigenvalues as a function of the CAP strength parameter λ , with $\lambda_j = 0.0001(j-1)$. The basis set consists of 60 even-tempered Gaussian functions. The continuous line stands for the numerically exact results obtained with complex rotation. A comparison of these results with those displayed in Fig. 2 shows that for the even-tempered Gaussian basis set the complex eigenvalues converge more slowly than for the particle-in-a-box basis functions since the critical value of λ is about ten times larger. The arrow selects a representative value of λ . R stands for the resonance position.

are given in Table I, calculated with the continued fraction procedure [28]. The results are of good quality only when both polynomials in the ratio have equal degrees ($M+N$ even in the table). There is no obvious explanation for this behavior. The good stability of results for this choice can serve as a criterion.

V. CONCLUDING REMARKS

It is shown here that the exponentially diverging resonance wave functions become square integrable when *any* complex absorbing potential $-i\lambda r^N$ with $N \geq 0$ is added to the system Hamiltonian. For a multidimensional Hamiltonian the CAP should be written $-i\lambda r^N$. This happens even when λ gets infinitesimally small values. Because the integration range or the basis sets are necessarily finite λ should in practice exceed a critical value λ_c to produce the so-called exact λ -dependent energies. The value of λ_c starts to decrease as

the calculation is made more accurate by extending the integration range and $E(\lambda_c)$ gets closer to the resonance energy. However, another route to estimate the resonance positions and lifetimes is to apply the Padé approximation which bridges the gap between $\lambda = \lambda_c$ and $\lambda = 0$. This approach might be found most attractive when one wishes to compute resonances with the help of widely used conventional numerical packages that were developed for the calculations of bound states.

APPENDIX: ASYMPTOTIC BEHAVIOR OF A WAVE FUNCTION WITH A LINEAR IMAGINARY POTENTIAL

The wave equation with a linear imaginary potential is (in a.u.)

$$\left(-\frac{1}{2m} \frac{\partial^2}{\partial r^2} + V(r) - i\lambda r - E\right) \Psi(r) = 0. \quad (\text{A1})$$

For large r , after $V(r)$ has vanished, the wave equation becomes locally

$$\left(-\frac{1}{2m} \frac{\partial^2}{\partial r^2} - i\lambda r - E\right) \Psi(r) = 0. \quad (\text{A2})$$

A change of variables is made to bring it to a standard form:

$$z = (2m\lambda)^{1/3} \left(ir + \frac{E}{\lambda}\right) \quad (\text{A3})$$

giving

$$\left(\frac{\partial^2}{\partial z^2} - z\right) \Psi(z) = 0. \quad (\text{A4})$$

This equation has for solutions the Airy functions $\text{Ai}(z)$ and $\text{Bi}(z)$ [29]. For $r \rightarrow \infty$, we can use the expressions of $\text{Ai}(z)$ and $\text{Bi}(z)$ for a large modulus of z [Eqs. (10.4.59) and (10.4.63) of [29]]:

$$\text{Ai}(z) \sim \frac{1}{2} \frac{1}{\sqrt{\pi}} z^{-1/4} e^{-(2/3)z^{3/2}}, \quad (\text{A5})$$

$$\text{Bi}(z) \sim \frac{1}{\sqrt{\pi}} z^{-1/4} e^{+(2/3)z^{3/2}}. \quad (\text{A6})$$

For large r , z is dominated by the first term. We have:

TABLE I. Extrapolated energies with the Padé procedure applied to the energies obtained with a Gaussian basis. A continued-fraction method [28] is used here. M is the degree of the polynomial in the denominator while N is for the numerator. For $M+N$ even $M=N$, while for $M+N$ odd $M=N+1$.

$M+N$	$\text{Re}(E_{Res})$	$\text{Im}(E_{Res})$	$M+N$	$\text{Re}(E_{Res})$	$\text{Im}(E_{Res})$
2	1.32552093	-0.0157077128	9	1.32716684	-0.0176695815
3	1.3155404	-0.0255419827	10	1.32571199	-0.0158415378
4	1.3256868	-0.0157609616	11	1.32828364	-0.0134598865
5	1.31687519	-0.0184641115	12	1.32572353	-0.0158482468
6	1.32571613	-0.0158047955	13	1.32543153	-0.0122016644
7	1.32959555	-0.0197172829	14	1.32563783	-0.0158178091
8	1.32571468	-0.0158431948			

$$z^{3/2} \sim (m\lambda)^{1/2} r^{3/2} (i-1). \quad (\text{A7})$$

This gives for the asymptotic forms of $\text{Ai}(z)$ and $\text{Bi}(z)$

$$\text{Ai}(z) \sim \frac{1}{2} \frac{1}{\sqrt{\pi}} \left(ir + \frac{E}{\lambda} \right)^{-1/4} e^{-(2i/3)r^{3/2}} e^{+(2/3)(m\lambda)^{1/2} r^{3/2}}, \quad (\text{A8})$$

$$\text{Bi}(z) \sim \frac{1}{\sqrt{\pi}} \left(ir + \frac{E}{\lambda} \right)^{-1/4} e^{+(2i/3)r^{3/2}} e^{-(2/3)(m\lambda)^{1/2} r^{3/2}}. \quad (\text{A9})$$

We observe that $\text{Ai}(z)$ is a progressive wave function running to the left, with a diverging factor for $r \rightarrow +\infty$, while $\text{Bi}(z)$ is running to the right and is damped. Thus $\text{Bi}(z)$ is the function with the correct boundary condition. A linear imaginary potential produces a localization of the wave function. Another route to this result is to use semiclassical theory. This is done in the text for a CAP of the general form $-i\lambda r^N$. For $N=1$ one recovers exactly the result given by the Airy function.

-
- [1] L. S. Cederbaum, J. Zobeley, and F. Tarantelli, *Phys. Rev. Lett.* **79**, 4778 (1997); R. Santra and L. S. Cederbaum, *ibid.* **90**, 153401 (2003).
- [2] G. Öhrwall *et al.*, *Phys. Rev. Lett.* **93**, 173401 (2004); T. Jahnke *et al.*, *ibid.* **93**, 163401 (2004).
- [3] N. Moiseyev, S. Scheit, and L. S. Cederbaum, *J. Chem. Phys.* **121**, 722 (2004).
- [4] See, e.g., E. Garrido, D. V. Fedorov, and A. S. Jansen, *Nucl. Phys. A* **708**, 722 (2002).
- [5] J. H. Taylor, *Scattering Theory* (John Wiley, New York, 1972).
- [6] A. I. Baž, Ya. B. Zel'dovich, and A. M. Perelomov, *Scattering, Reactions and Decay in Nonrelativistic Quantum Mechanics* (Israel Program for Scientific Translations, Jerusalem, 1969); A. M. Perelomov and Ya. B. Zel'dovich, *Quantum Mechanics: Selected Topics* (World Scientific, Singapore, 1998).
- [7] C. Leforestier and R. E. Wyatt, *J. Chem. Phys.* **98**, 2334 (1983); **82**, 752 (1985).
- [8] For example, see E. Segré, *Nuclei and Particles* (Benjamin, New York, 1965), p. 467.
- [9] P. E. Hodgson, *The Optical Model of Elastic Scattering* (Clarendon Press, Oxford, 1963).
- [10] G. Jolicard and E. J. Austin, *Chem. Phys. Lett.* **121**, 106 (1985).
- [11] J. G. Muga, J. P. Palao, B. Navarro, and I. L. Egusquiza, *Phys. Rep.* **395**, 357 (2004), and references therein.
- [12] N. Moiseyev, *J. Phys. B* **31**, 1431 (1998).
- [13] U. V. Riss and H.-D. Meyer, *J. Phys. B* **31**, 2279 (1998).
- [14] E. Balslev and J. M. Combes, *Commun. Math. Phys.* **22**, 280 (1971).
- [15] B. Simon, *Commun. Math. Phys.* **27**, 1 (1972); *Phys. Lett.* **36A**, 23 (1971); *Ann. Math.* **97**, 247 (1973).
- [16] W. P. Reinhardt, *Annu. Rev. Phys. Chem.* **33**, 223 (1982).
- [17] N. Moiseyev and J. O. Hirschfelder, *J. Chem. Phys.* **88**, 1063 (1988).
- [18] N. Moiseyev, *Phys. Rep.* **302**, 211 (1998).
- [19] D. Neuhauser and M. Baer, *J. Chem. Phys.* **90**, 4351 (1989).
- [20] M. Child, *Mol. Phys.* **72**, 89 (1991).
- [21] A. Vibók and G. G. Balint-Kurti, *J. Chem. Phys.* **96**, 7615 (1992).
- [22] N. Lipkin, R. Lefebvre, and N. Moiseyev, *Phys. Rev. A* **45**, 4553 (1992).
- [23] R. Lefebvre, in *Resonances, Proceedings of the Lertorpet Meeting*, edited by E. Brändas and N. Elander (Springer, Berlin, 1988), p. 313.
- [24] N. Moiseyev, P. R. Certain, and F. Weinhold, *Mol. Phys.* **36**, 1613 (1978). See also Ref. [18], and references therein.
- [25] M. Rittby, N. Elander, and E. Brändas, *Phys. Rev. A* **26**, 1804 (1982); *Int. J. Quantum Chem.* **23**, 865 (1983).
- [26] H. J. Korsch, H. Laurent, and R. Möhlenkamp, *Phys. Rev. A* **26**, 1802 (1982).
- [27] O. Atabek and R. Lefebvre, *Nuovo Cimento Soc. Ital. Fis.*, **B 76B**, 176 (1983).
- [28] L. Schlessinger, *Phys. Rev.* **167**, 1411 (1966).
- [29] *Handbook of Mathematical Functions*, edited by M. Abramowitz and I. A. Stegun (Dover, New York, 1970).